

TURBULENCE SUSTAINED IN A PRECESSING SPHERE AND SPHEROIDS

Susumu Goto, Masahiro Fujiwara and Masahiro Yamato
Department of Mechanical Engineering,
Okayama University,
3-1-1, Tsushimanaka, Okayama, 700-8530, Japan
goto@mech.okayama-u.ac.jp

ABSTRACT

When a vessel filled with fluid is weakly precessing, developed turbulence is sustained in it. This interesting feature is quite attractive in engineering applications such as the effective turbulent mixing in a smooth cavity. The aim of our study is, for such applications, to clarify, experimentally, the suitable parameters (the rate of the precession, for example) and the effective shape of the vessel to produce strong turbulence.

Our previous laboratory experiments of fluid motions in a precessing sphere have shown that for Reynolds numbers Re (defined by the radius of the cavity, the magnitude of the spin angular velocity, and the kinematic viscosity of the fluid) larger than several thousands, turbulence can be sustained if the precession rate Γ (defined by the ratio of the magnitude of the precession angular velocity to that of the spin) is larger than 0.5 %, and it is most developed when Γ is about 5 %.

However, since only the viscous stress parallel to the wall produces turbulence in the spherical cavity, the shape is not necessarily the best to sustain strong turbulence effectively. Therefore, in the present study, we conduct experiments for flows in a precessing prolate spheroid. The result is, however, contrast to our intuition; that is, for a given Reynolds number, the minimum precession rate to sustain turbulence is significantly smaller in the precessing sphere than in the spheroid. This implies that the wall-normal stress does not enhance the turbulence, and that the precession of a symmetric cavity can produce more complex flows.

Furthermore, in order to investigate the influence of roughness of the cavity wall on the transition to turbulence, we investigate flows in the same prolate spheroid but with a step around the spin axis (the height of which is about $0.025a$, where a is the minor radius of the cavity). It is then shown that the flow dependence on Γ is hardly affected by this step. This result might imply that the transition to turbulence is due to the instability of the internal flow structures rather than those in the boundary layer.

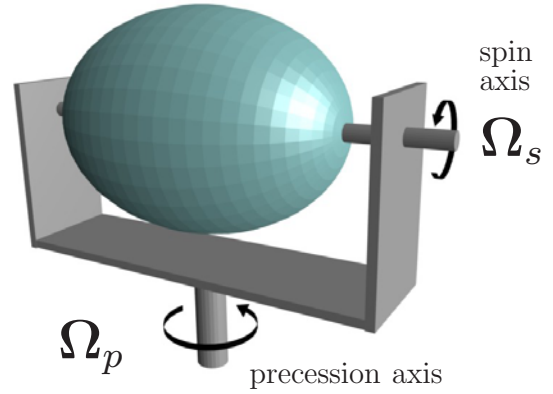


Figure 1. Precessing vessel. The precession axis is fixed in the laboratory, whereas the spin axis is fixed in the precession frame which rotates in a constant angular velocity Ω_p . In our experiments, the two axes are set in a right angle. The shown vessel is the prolate spheroid [shown in figure 3(b), below] with the ellipticity 0.9, where the major axis (polar axis) coincides with the spin axis.

Introduction

The precession is defined by the rotational motion of the spin axis of an object around another axis (the precession axis) which is not parallel to the spin axis. An example of a precessing object is shown in figure 1. In the present study, we restrict ourselves within the case that the spin and the precession axes are perpendicular to each other as shown in this example. The fact that weak precession of a vessel produces strong turbulence of the confined fluid is contrast to our general experience that it is rather difficult to sustain a turbulent flow inside a smooth cavity only by its rotational motion; recall the fact that the solid-body rotational flow of the confined fluid is always established by the steady rotation of an any-shaped cavity.

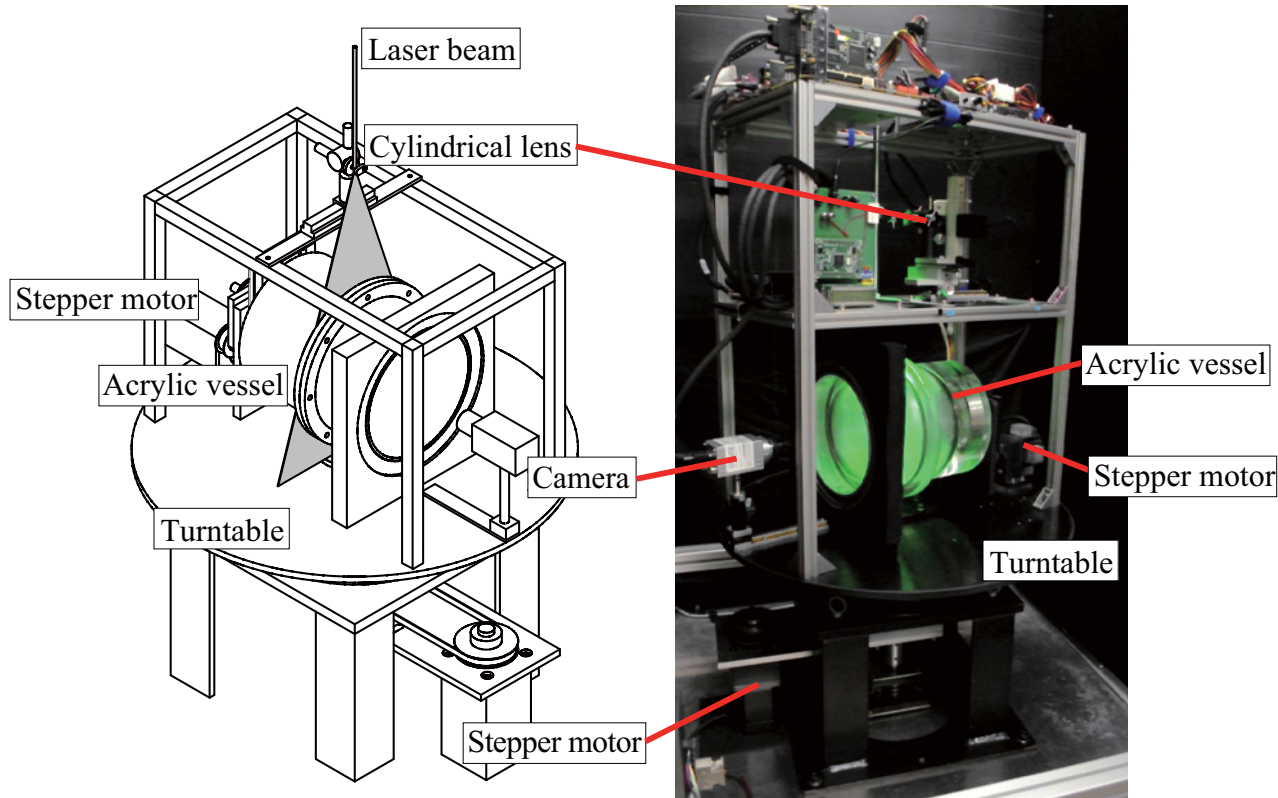


Figure 2. Experimental apparatus. The precession of the vessel (the outer shape of which is cylindrical) is driven by a pair of stepper motors. The light source for visualisations and measurements is the laser sheet on the plane perpendicular to the spin axis. The incident laser beam goes along the precession axis, and the laser sheet is produced by the cylindrical lens fixed on the turntable.

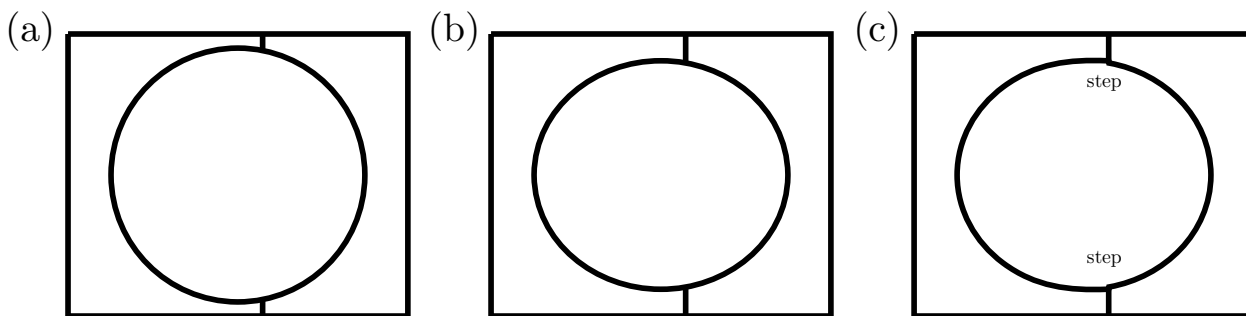


Figure 3. Vessels used in the experiments. The cylindrical outer shape is common, whereas the shape of the cavity is (a) a sphere (radius is 90 mm) and (b,c) a prolate spheroid (ellipticity is 0.9, major radius is 90 mm). The cavity (c) is the same as in (b) but with a 2 mm height step on the cavity wall. Each vessel consists of two parts. The cross-section on the plane spanned by the spin and the precession axes is shown.

Because the spin axis of the Earth slowly precesses with the period of about 27 000 years, since the seminal experiment by Malkus (1968) and theoretical work by Busse (1968), quite a few geophysicists have been interested in the potential ability of the weak precession to produce turbulence of melted iron in the outer core (Vanyo, 1991; Vanyo *et al.*, 1995; Vanyo

& Dunn, 2000; Noir *et al.*, 2003; Cardin & Olson, 2007), especially from the point of view of the sustaining mechanism of the geomagnetic fields (Kerswell, 1996; Tilgner, 1999, 2005, 2007; Wu & Roberts, 2009). However, this simple mechanism to sustain strong turbulence has not been emphasised in engineering, although its wide applications to mixers without

stirrers, chemical reaction chambers, food processors, and so on are expected.

For such applications, in this article we aim at revealing the parameter dependence of flow structures in a precessing cavity. It can be shown from the Navier-Stokes equations for an incompressible viscous fluid that, once we fix the angle between the spin and precession axes, only the following two parameters

$$Re = \frac{a^2 \Omega_s}{\nu} \quad (\text{Reynolds number}) \quad (1)$$

and

$$\Gamma = \frac{\Omega_p}{\Omega_s} \quad (\text{precession rate}), \quad (2)$$

which is sometimes called the Poincaré number, control the flow in a precessing cavity. Here, we have employed the radius a of the sphere (or the minor radius of the spheroid) and the reciprocal of the spin angular velocity Ω_s as characteristic length and time, respectively to define the Reynolds number (1); and ν is the kinetic viscosity of the fluid. In (2), Ω_p is the magnitude of the precession angular velocity. It was recently shown (Goto *et al.*, 2007, 2011) by conducting a systematic series of experiments of turbulence in a precessing *sphere* that the strongest turbulence is sustained when the precession rate is very weak such as $\Gamma \approx 0.05$ and the maximum Taylor-length based Reynolds number is about \sqrt{Re} .

However, a possible objection of these experiments is in the choice of the cavity shape. More concretely, since a sphere does not change its shape by its precession, the wall-normal stress cannot play a role to produce turbulence in the cavity. Hence, other asymmetric shapes are likely to be more effective to sustain stronger turbulence. Therefore, in the present study, we conduct experiments using a precessing spheroid (a prolate spheroid with the ellipticity 0.9), and compare the results with those for the precessing sphere.

Experimental setup

It is not difficult to drive the precession of a vessel such as shown in figure 1 in the laboratory. The precession may be driven by rotating a vessel in a constant angular velocity Ω_s on the turntable which rotates in a constant angular velocity Ω_p . For this purpose, we have constructed an apparatus depicted in figure 2.

In our experiments, the two rotational motions are driven by a pair of stepper motors, and the working fluid is degassed tap water. As stressed in the previous section, this system is controlled only by the Reynolds number (1) and the precession rate (2). Therefore, the excellent reproducibility of experiments is assured as long as the kinematic viscosity ν of the fluid and the magnitudes Ω_s and Ω_p of two angular velocities are precisely determined. For the former, we monitor the temperature of the fluid by an accurate thermistor embedded in the vessel; and for the latter, we use precise pulse generators and stepper motors with sufficiently small step angles.

The light source of flow visualisations and measurements is a laser sheet, which runs through the centre of the cavity

in the perpendicular direction to the spin axis. As shown in figure 2, the incident laser beam runs along the precession axis, and it is fanned out by the cylindrical lens fixed on the turntable. By this mechanism, the laser sheet rotates together with the turntable. Then, the reflected light by the particles on this laser sheet are recorded by a digital camera fixed on the table. In other words, all the flow visualisations and measurements are conducted in the frame (the precession frame) rotating with the turntable. Note that the boundary conditions and the governing equations for the confined fluid are time-independent in the precession frame. Therefore, as seen below (figure 4), flow in the cavity is steady in this frame of reference, when the precession rate Γ is small.

As also shown in figure 2, the outer shape of the vessel is cylindrical, whereas shapes of the cavity is spherical or spheroidal. More precisely, we use the three different cavities shown in figure 3; (a) a spherical cavity (the radius is 90 mm), (b) a spheroidal cavity (a prolate spheroid, the polar axis of which coincides with the spin axis, the ellipticity is 0.9, and the major radius is 90 mm), and (c) the same spheroidal cavity as in (b) but with a step of about 2 mm on the cavity wall.

By the use of a large bearing to support the spin axis, a flat observation window is set at the bottom of the cylindrical vessel, which is made of acrylic (the refractive index is 1.49), and the images are taken by the digital camera from the perspective along the spin axis. It is then verified by taking the image of reference grids on the visualised plane that the distortion of images are negligibly small especially in the central region on the measurement plane.

The flow visualisations (shown in figures 4 and 6, below) are conducted by the suspension of reflective flakes. Here, the flakes we use are thin flat particles, the size of which is about $(10\mu\text{m})^2 \times 0.1\mu\text{m}$. A small amount (0.04 g) of flakes are seeded in the water of about 3.0 kg in the cavity.

Flow dependence on the precession rate

First, we investigate the flow dependence on the precession rate (2). The results of flake visualisations at a fixed Reynolds number, $Re = 8.0 \times 10^4$, are shown in figure 4(a) for the sphere, and in figure 4(b) for the spheroid.

It is interesting that the qualitative parameter dependence is common both in the cases of the sphere and the spheroid as summarised in the following:

1. For $\Gamma = 0$, the solid-body rotational flow is established [figures 4(a1,b1)].
2. For very small precession rates, steady flows are sustained, in which clear stationary patterns are observed [figures 4(a2, b2)]. It may be worth mentioning, in passing, that the boundary layer theory (see Kida 2011) and direct numerical simulation show that the steady flow observed in figure 4(a2) consists of the inclined solid-body rotational flow accompanied with a pair of conical internal shear layers.
3. For slightly larger Γ , a periodic flow is observed [figures 4(a3, b3)]. The instability of the steady flow seems to be triggered in the central region of the cavity. Note that the periodic flow (b3) in the spheroid is observed around $\Gamma = 0.03$, which is ten times larger than in (a3), $\Gamma =$

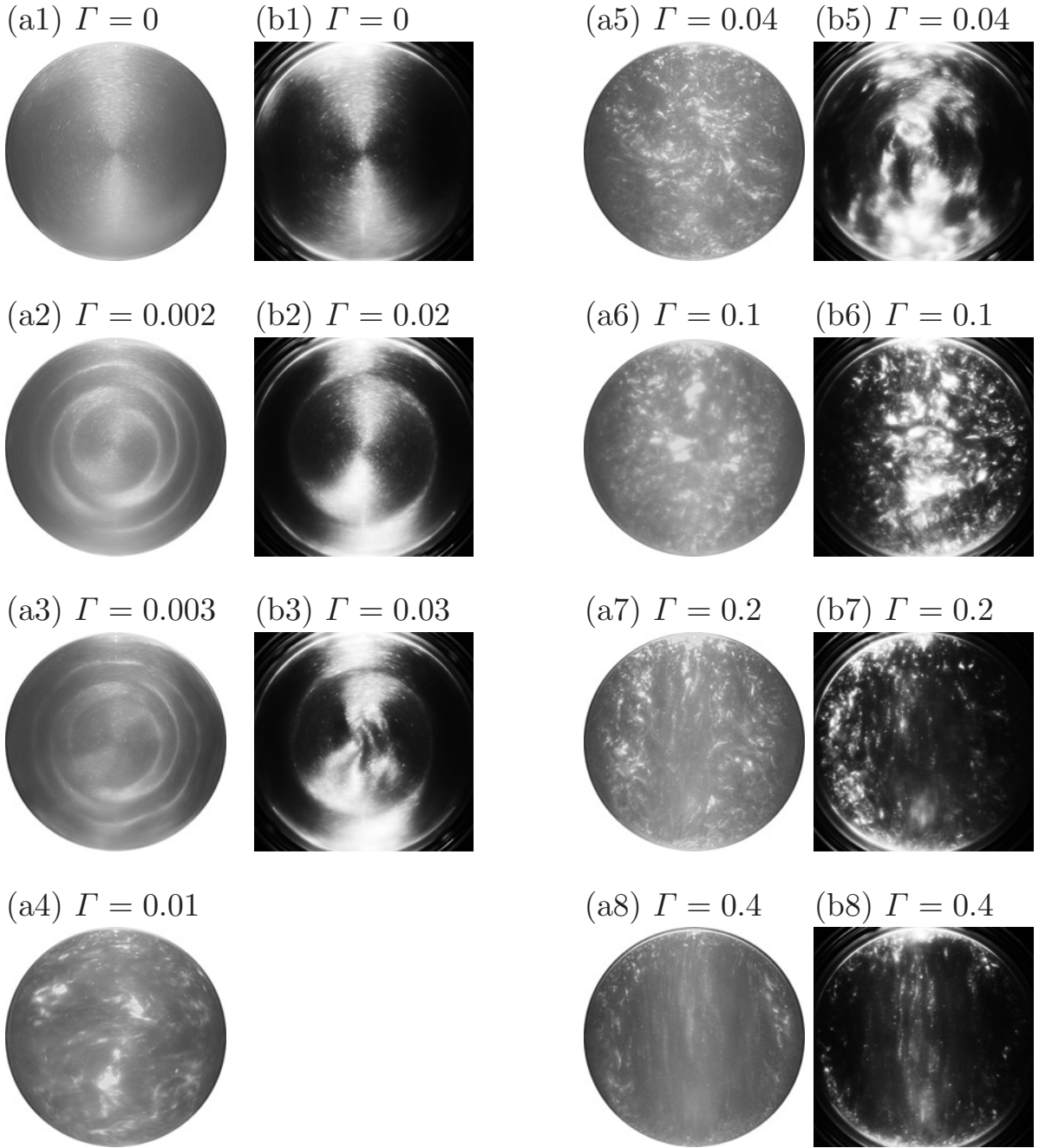


Figure 4. Flow visualisations by reflective flakes in (a) the precessing sphere, and in (b) the precessing prolate spheroid. The Reynolds number Re is fixed at 8.0×10^4 , and the flow dependence on the precession rate Γ is investigated. In (a1,b1), the solid-body rotational flows around the spin axis are established. The steady flows observed in (a2) and (b2) become unstable at the precession rate shown in (a3) and (b3) to be periodic flows, respectively. The flows shown in (a4–a8,b5–b8) are turbulence; though turbulence is confined only in the outer region for the stronger precession cases (a7, a8, b7, b8).

0.003, for the sphere.

4. For larger Γ , turbulence is sustained; for relatively small Γ , the circulation around the spin axis dominates [figures 4(a4, b5)], whereas almost isotropic turbulence is sustained for larger Γ [figures 4(a5, a6, b6)].
5. For larger Γ , turbulence is weaker, and confined within

the outer region. Whereas, in the inner region, laminar flow appears due to the rapid turntable rotation [figures 4(a7, a8, b7, b8)].

6. For larger Γ (≈ 1), the flow tends to the solid-body rotational flow about the precession axis, and no fluid motion except in the thin boundary layer is observed in the pre-

cession frame.

Although the qualitative feature of the transition from laminar flows to turbulence is quite common in the both cavities, the critical values of the transition are significantly different. The comparison between figures 4(a) and (b) shows that weaker precession can produce turbulence in the precessing sphere than in the spheroid. More detailed parameter surveys show that $\Gamma \approx 0.004$ is sufficient for the former cavity, but $\Gamma \gtrsim 0.04$ is needed for the latter at this Re to sustain turbulence. Indeed, developed turbulence is observed in the sphere when $\Gamma = 0.01$ [figure 4 (a4)], but a steady flow accompanied with a stationary pattern is observed in the spheroid at the same precession rate $\Gamma = 0.01$ [figure 4 (b2)].

The qualitatively same flow dependence on Γ as in figure 4 is observed for different Reynolds numbers in the range $O(10^3) < Re < O(10^5)$.

Minimum precession rate to sustain unsteady flows

Next, we investigate the dependence on Re of the critical precession rate Γ_c to sustain unsteady flows. We plot, in figure 5, the boundary between the steady flows (open symbols) and the unsteady flows (closed symbols). Circles and squares denote the sphere and spheroid cases, respectively. It is clearly observed in this figure that turbulence is more easily (at weaker precession rates) sustained in the sphere than the spheroid. More precisely, figure 5 shows that the critical values of the precession rate Γ_c to sustain an unsteady flow is

$$\Gamma_c^{(\text{sphere})} \sim Re^{-0.9} \quad (3)$$

for the sphere, whereas

$$\Gamma_c^{(\text{spheroid})} \sim Re^{-0.4} \quad (4)$$

for the spheroid. These imply that in a huge Reynolds-number system (such as in the outer core of the Earth, or industrial mixing chambers), a spherical cavity is much more effective to sustain turbulence than the spheroid.

Roughness of the cavity wall

Before closing the present article, we report the experiments on the influence of the roughness of the cavity wall. As shown in figure 3, for a technical reason, each of the cavities used in our experiments consists of two parts. This implies that there is a small step on the cavity wall. The height of the step, which is approximately symmetric about the spin axis, is the order of the machining tolerance ($0.1 \text{ mm} \approx 0.001a$). However, since the boundary layer thickness is also quite small, it might affect the critical number of the precession rate Γ to sustain turbulence.

To investigate the influence of the small step, we conduct experiments of the flow in a precessing spheroid [figure 3(c)] with a large step, the height of which is about $2 \text{ mm} \approx 0.025a$.

For the given Reynolds number, $Re = 4.0 \times 10^4$, flow visualisations for the precession rates $\Gamma = 0.03, 0.032$ and 0.034

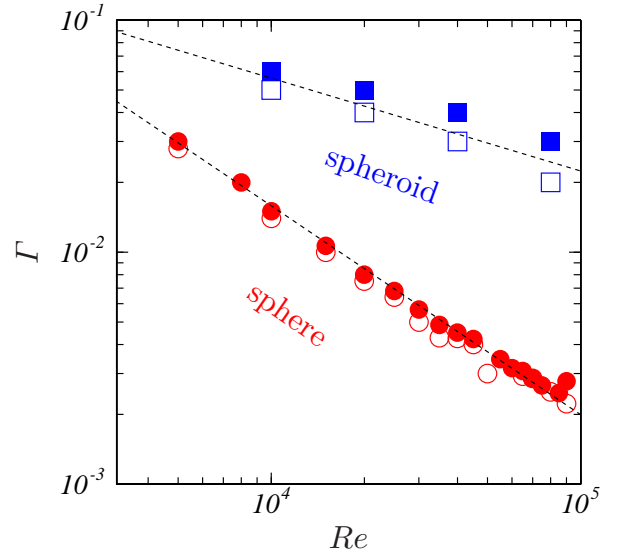


Figure 5. Boundary between the steady flows (\circ for the sphere, \square for the spheroid) and unsteady flows (\bullet for the sphere, \blacksquare for the spheroid). The horizontal and vertical axes are the Reynolds number Re and the precession rate Γ , respectively. It is seen that, for a given Reynolds number, weaker precession can sustain unsteady flows in the sphere than in the spheroid. Dotted lines indicate $Re^{-0.9}$ and $Re^{-0.4}$.

are shown in figure 6; where (a) is the results for the spheroid without the step, and (b) is for with it. No qualitative difference between (a) and (b) is observed. In the both cases, when $\Gamma = 0.03$ a steady flow with a stationary pattern is observed; when $\Gamma = 0.032$ an instability of the steady flow takes place in the central region; and when $\Gamma = 0.034$, the instability becomes more noticeable.

This result assures that such a small step on the cavity wall, which is inevitable in our experiments, has no influence on the critical value of the precession rate to sustain turbulence. Furthermore, it implies that the instability to produce turbulence may well occur in the internal flow rather than in that in the boundary layer, although this is not conclusive because, here, only the step symmetric about the spin axis has been investigated.

Conclusion

The most remarkable conclusion of the present study is that *turbulence is more easily sustained in the precessing sphere than in the precessing spheroid*. This experimental fact is scientifically interesting because it seems contradictory to our intuition. It is also important in geophysics, since the Earth is a spheroid. Furthermore, it is encouraging from the viewpoint of applications because a simpler shaped cavity makes more complex fluid motions. Although the physical reason of this controversial conclusion is unknown, the axisymmetric mode might be the most unstable, and the asymmetry of the spheroid could be a disadvantage for the instability to grow.

We are now conducting a series of systematic measurements by particle image velocimetry, as well as direct nu-

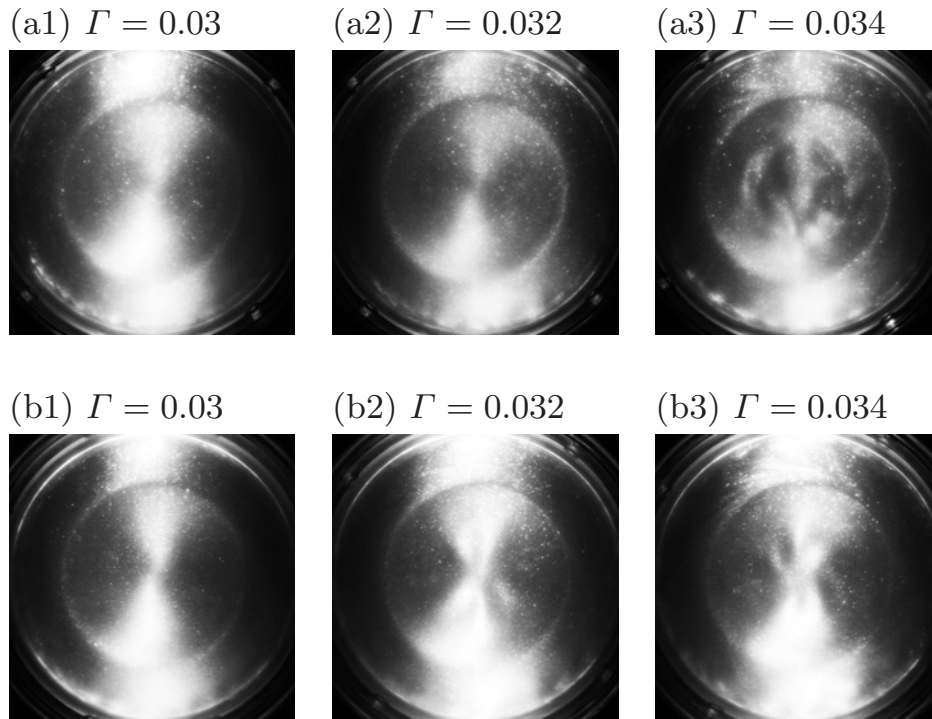


Figure 6. Flake visualisations of flows in (a) the smooth prolate spheroid, and in (b) the spheroid with a step on the cavity wall. The Reynolds number is fixed at 4.0×10^4 . No qualitative difference between the two cases is observed. The both flows are steady with the similar stationary pattern at the precession rate $\Gamma = 0.03$, and these flows become unstable in the central region at $\Gamma = 0.032$ (the instability is more conspicuous at $\Gamma = 0.034$).

merical simulations; and we shall report more quantitative results based on the these experiments and numerical simulations elsewhere in the near future.

This work was partly supported by Japan Society for the Promotion of Science, Grant-in-Aid for Young Scientists (21760130).

REFERENCES

- Busse, F. H. 1968 Steady fluid flow in a precessing spheroidal shell. *J. Fluid Mech.* **33**, 739–751.
- Cardin, P. & Olson, P. 2007 Experiment on core dynamics. *Core dynamics of Treatise of Geophysics* **8**, 319–345.
- Goto, S., Ishii, N., Kida, S. & Nishioka, M. 2007 Turbulence generator using a precessing sphere. *Phys. Fluids* **19**, 061705.
- Goto, S., Matsunaga, A., Nishioka, M., Kida, S. & Tsuda, S. 2011 Turbulence sustained in a precessing sphere (to be submitted).
- Kerswell, R. R. 1996 Upper bounds on the energy dissipation in turbulent precession. *J. Fluid Mech.* **321**, 335–370.
- Kida, S. 2011 Steady flow in a rapidly rotating sphere with weak precession. *J. Fluid Mech.* (in press).
- Malkus, W. V. R. 1968 Precession of the earth as the cause of geomagnetism. *Science* **160**, 259–264.
- Noir, J., Cardin, P., Jault, D. & Masson, J.-P. 2003 Experimental evidence of nonlinear resonance effects between retrograde precession and the tilt-over mode within a spheroid. *Geophys. J. Int.* **154**, 407–416.
- Tilgner, A. 1999 Magnetohydrodynamics flow in precessing spherical shells. *J. Fluid Mech.* **379**, 303–318.
- Tilgner, A. 2005 Precession driven dynamos. *Phys. Fluids* **17**, 034104.
- Tilgner, A. 2007 Kinematic dynamos with precession driven flow in a sphere. *Geophys. Astrophys. Fluid Dyn.* **101**, 1–9.
- Vanyo, J., Wilde, P., Cardin, P. & Olson, P. 1995 Experiments on precessing flows in the earth’s liquid core. *Geophys. J. Int.* **121**, 136–142.
- Vanyo, J. P. 1991 A geodynamo powered by luni-solar precession. *Geophys. Astrophys. Fluid dyn.* **59**, 209–234.
- Vanyo, J. P. & Dunn, J. R. 2000 Core precession: flow structures and energy. *Geophys. J. Int.* **142**, 409–425.
- Wu, C. C. & Roberts, P. H. 2009 On a dynamo driven by topographic precession. *Geophys. Astrophys. Fluid Dyn.* **103**, 467–501.